Inhibition of Bcl-2 and Bcl-xL overcomes the resistance to the third-generation EGFR tyrosine kinase inhibitor osimertinib in non-small cell lung cancer

YINGJIE LU[1,2], DONGLIANG BIAN[1,2], XUELIN ZHANG[1,2], HUIBIAO ZHANG[1,2] and ZHENGHONG ZHU[1,2]

[1]Department of Thoracic, [2]Shanghai Key Laboratory of Clinical Geriatric Medicine, Huadong Hospital Affiliated to Fudan University, Shanghai 200040, P.R. China

Received February 7, 2020; Accepted October 2, 2020

DOI: 10.3892/mmr.2020.11686

Abstract. Epidermal growth factor receptor (EGFR) tyrosine kinase inhibitors (TKIs) have demonstrated significant benefits to patients with non-small cell lung cancer (NSCLC) harboring EGFR-activating mutations; however, acquired resistance limits their long-term efficacy. Therefore, it remains an urgent requirement to discover the underlying mechanisms and investigate novel therapeutic strategies for overcoming the resistance to EGFR TKIs. The present study aimed to determine the mechanism underlying the resistance of NSCLC cells to osimertinib, a third-generation EGFR tyrosine kinase inhibitor, the osimertinib-resistant NSCLC cell sub-line HCC827/OR was established in the present study. It was found that the expression levels of Bcl-2 and Bcl-xL were significantly upregulated in resistant cells compared with sensitive cells. Furthermore, the suppression of Bcl-2 and Bcl-xL through small interfering RNA-mediated gene knockdown or using a small molecule specific inhibitor ABT-263 re-sensitized HCC827/OR cells to osimertinib treatment. Moreover, the combined treatment of HCC827/OR cells with ABT-263 and osimertinib enhanced the rate of cell apoptosis through the mitochondrial apoptotic pathway. Finally, ABT-263 was able to overcome the resistance of osimertinib in xenograft tumor models. In conclusion, these findings may provide an improved concept for the development of a novel combined therapeutic strategy for the treatment of NSCLC resistance to EGFR TKIs.

Introduction

Non-small cell lung cancer (NSCLC), which represents ~80% of all lung cancers, is the most common type of cancer and the leading cause of cancer-related deaths worldwide (1,2). Epidermal growth factor receptor (EGFR)-activating mutations have been identified in 15-40% of patients with NSCLC and have emerged as an effective therapeutic target (3). In fact, the first-generation EGFR tyrosine kinase inhibitors (TKIs), such as gefitinib and erlotinib, were discovered and recommended as a standard therapy for patients with advanced NSCLC and EGFR-sensitive mutations (4-6). However, despite the initial significant response to the treatment with TKIs, acquired resistance develops in the majority of patients with NSCLC within a median time of 10-16 months, which limits the long-term efficacy of TKIs (7). The acquisition of a secondary T790M mutation in exon 20 of EGFR, which occurs in ~60% of resistant cases, is the most commonly characterized mechanism underlying the acquired resistance to the first-generation of EGFR TKIs (8). To overcome the resistance induced by the T790M mutation, osimertinib, as a third-generation EGFR TKI, was developed and demonstrated a beneficial efficacy in patients with NSCLC carrying the resistant T790M mutation of EGFR (9,10). Unfortunately, similar to other EGFR TKIs, the efficacy of osimertinib is limited due to acquired resistance arising from multiple mechanisms, including the EGFR C797S mutation and activation of parallel signaling pathways, amongst others (11,12). Therefore, there remains an urgent requirement to discover the underlying mechanisms of resistance and investigate novel therapeutic strategies for overcoming the recurring resistance to osimertinib.

Recently, increasing evidence has revealed that NSCLC cells develop resistance to EGFR TKIs via inhibition of cellular apoptosis by modulating apoptotic regulators belonging to the Bcl-2 family (13,14). Among these, Bcl-2 and Bcl-xL, which are EGFR/AKT downstream antiapoptotic signaling proteins, have been identified to be responsible for the drug resistance in numerous types of tumor, such as small-cell lung (15), breast (16) and ovarian cancers (17).

The present study aimed to determine whether the dysregulation of Bcl-2 and Bcl-xL was involved in the resistance of NSCLC cells to osimertinib through establishing an osimertinib-resistant NSCLC cell sub-line, HCC-827/OR. The results revealed that the expression levels of Bcl-2 and Bcl-xL were upregulated in HCC-827/OR cells. Moreover, ABT-263, a small molecular inhibitor of Bcl-2 and Bcl-xL, was discovered

Correspondence to: Professor Zhenghong Zhu, Department of Thoracic, Huadong Hospital Affiliated to Fudan University, 221 West Yan'an Road, Shanghai 200040, P.R. China
E-mail: drzhuzhenghong@163.com

Key words: non-small cell lung cancer, osimertinib resistant, ABT-263, Bcl-2, Bcl-xL

to exert synergetic antitumor effects with osimertinib in HCC-827/OR cells *in vitro* and *in vivo*. Overall, these findings may provide a potential therapeutic strategy to overcome the resistance of NSCLC to osimertinib.

Materials and methods

Cell lines and reagents. The NSCLC cell line HCC827 was obtained from The Cell Bank of Type Culture Collection of the Chinese Academy of Sciences. Cells were cultured at 60-90% confluence in RPMI-1640 medium (Thermo Fisher Scientific, Inc.), supplemented with 10% FBS (Thermo Fisher Scientific, Inc.) and 1% penicillin-streptomycin, and maintained at 37˚C in a humidified incubator with 5% CO_2. Osimertinib-resistant HCC827 cell line (HCC-827/OR) was established beginning with exposing HCC827 parent cells to a culture medium with 5 nM osimertinib. When the cells were resistant to 5 nM osimertinib, the concentration was increased to 10 nM. During over a period of 6 months, the cells were stably grown in a culture medium containing 100 nM osimertinib. Osimertinib and ABT-263 were purchased from MedChemExpress and Sigma-Aldrich (Merck KGaA), respectively. Both drugs were dissolved in DMSO and stored at -20˚C. MTT reagent was purchased from Sigma-Aldrich (Merck KGaA).

Cell viability assay. The inhibitory effects of osimertinib or ABT-263 on cell viability were evaluated using an MTT assay. Briefly, cells were seeded in 96-well plates (5x10^3 cells per well) and treated with osimertinib, ABT-263 and osimertinib and ABT-263 together at 1, 2.5, 5 or 10 μM, respectively, or DMSO as the negative control for 24 h. Then, the medium containing the drugs or DMSO was replaced with fresh medium containing 0.5 mg/ml MTT and incubated for 4 h at 37˚C. Following the incubation, the MTT-containing medium was discarded, and 150 μl DMSO was added to each well to dissolve the formazan and shook for 15 min in the dark. The absorbance at 570 nm was determined using a microplate reader (Synergy H4; BioTek Instruments, Inc.).

Flow cytometric analysis of apoptosis. Cellular apoptosis was analyzed using an Annexin V-FITC/PI Apoptosis Detection kit (BD Biosciences), according to the manufacturer's protocol. Briefly, cells were incubated with the indicated concentrations of osimertinib, ABT-263, osimertinib and ABT-263, or DMSO as the negative control for 24 h. The cells were subsequently trypsinized, washed and resuspended in 200 μl binding buffer, then stained with 5 μl PE and FITC for 15 min in the dark at room temperature. Finally, the stained cells were subjected to analysis by flow cytometry (Cytomics FC 500 MPL; Beckman Coulter, Inc.). The obtained data were analyzed by CytExpert v2.3 (Beckman Coulter, Inc.). The early apoptosis was evaluated based on the percentage of cells with Annexin V^+/PI^-, while the late apoptosis was that of cells with Annexin V^+/PI^+. The results are presented as the mean ± SD of three independent experiments.

Small interfering RNA (siRNA)-mediated knockdown of gene expression. Bcl-2, Bcl-xL and Bcl-2-like protein 11 (Bim) siRNA or control siRNA were purchased from Shanghai GenePharma Co., Ltd., and transfected into cells using Lipofectamine® 2000 (Invitrogen; Thermo Fisher Scientific, Inc.), according to the manufacturer's protocol. Briefly, cells were seeded in the 6-well plates (1x10^5 cells/ml) with growth medium without antibiotics 1 day before transfection, such that they will be 30-50% confluence at the time of transfection. For each transfection sample, the transfection complex was prepared by dilution of 100 pmol siRNA oligomer and 5 μl Lipofectamine 2000 with 250 μl Opti-MEM medium (Thermo Fisher Scientific, Inc.) without serum, which was added to each well. After incubation at 37˚C in a CO_2 incubator for 8-10 h, the cultured medium containing siRNA and transection agent was replaced with fresh medium. To confirm the downregulation of the expression levels of the target proteins, cells were collected and lysed 48 h after transfection, and western blotting or reverse transcription-quantitative PCR (RT-qPCR) was used to confirm the transfection efficiency. The following siRNA sequences (Thermo Fisher Scientific, Inc.) were used: Bcl-2 sense, 5'-GGAUGACUGAGUACCUGAAdTdT-3' and antisense, 3'-dTdTCCUACUGACUCAUGGACUU-5' (14); Bcl-xL sense, 5'-GGUAUUGGUGAGUCGGAUCdTdT-3' and antisense, 3'-dTdTCCAUAACCACUCAGCCUAG-5' (18); Bim sense, 5'-AAUUGU CUACCUUCUCGGUdTdT-3' and antisense, 3'-dTdTUUAACAGAUGGAAGAGCCA (19); and control siRNA sense, 5'-UUCUCC GAACGUGUCACGUTT-3' and antisense, 5'-ACGUGACACGUUCGGAGAATT-3'.

Western blotting. Cells were harvested and lysed with RIPA lysis buffer (Beyotime Institute of Biotechnology). Total protein concentration was determined using a BCA protein assay kit (Beyotime Institute of Biotechnology) and 30 μg protein/lane was separated by 12% SDS-PAGE. The separated proteins were transferred onto PVDF membranes (EMD Millipore) and blocked by 5% skimmed milk for 1 h at room temperature. The membranes were then incubated with primary antibodies (diluted 1:1,000 with 1% skimmed milk for Bcl-2, Bcl-xL, BimEL, cytochrome *c*, cleaved- and full length PARP-1 and caspase-3, and diluted 1:10,000 with 1% skimmed milk for β-actin) overnight at 4˚C, followed by incubation with a horseradish peroxidase (HRP)-conjugated secondary antibody (1:5,000 diluted by TBST) for 1 h at room temperature. Protein bands were visualized using an ECL reagent (EMD Millipore). β-actin was used as an endogenous loading control. ImageJ (version 1.48; National Institutes of Health) was used to analyze the grey level of the bands. Representative data from ≥3 independent experiments are presented. Primary antibodies against Bcl-2 (cat. no. 12789-1-AP), Bcl-xL (cat. no. 26967-1-AP), BimEL (cat. no. 22037-1-AP), cytochrome *c* (cat. no. 10993-1-AP) were purchased from ProteinTech Group, Inc. Primary antibody against cleaved poly(ADP-ribose) polymerase-1 (PARP-1; cat. no. sc-56196), PARP-1 (cat. no. sc-74470) and caspase-3 (cat. no. sc-7272) were purchased from Santa Cruz Biotechnology, Inc. Primary antibodies targeting β-actin (cat. no. 4970) and cleaved caspase-3 (cat. no. 9664) and HRP-conjugated secondary antibody (cat. nos. 7074 and 7076) were purchased from Cell Signaling Technology, Inc.

Colony formation assay. A total of 1x10^3 cells/well were seeded into 6-well plates at a single cell density and treated with osimertinib or/and ABT-263 or DMSO (negative control) at the indicated concentrations for 48 h. The drug-containing medium was replaced with fresh medium and cells were cultured for 2 weeks. Then the cells were fixed with methanol for 15 min at room temperature, followed by staining with gentian violet (Beijing Solarbio Science & Technology Co., Ltd.) for 1 h at room temperature. The colonies with >50 cells were counted under an inverted microscope (IX71; Olympus Corporation; magnification, x10).

Xenograft study. The animal experimental protocol was approved by the Animal Ethics Committee of Fudan University Shanghai Medical School (Shanghai, China). A total of 24 female BALB/c nude mice (age, 6-7 weeks; weight 20±2 g) were purchased from Shanghai SLAC Laboratory Animal Co., Ltd., and housed in a specific pathogen-free environment under a 12-h light-dark cycle at 23±1˚C and 50±5% humidity atmosphere, with free access to standard food and water. A total of $5x10^6$ HCC827/OR cells/mouse resuspended in 200 μl PBS were subcutaneously implanted into the right flank of nude mice. The tumor volume was measured using a digital caliper and calculated using the following formula: Volume = L x S^2 x 0.52, where L represents the longest tumor diameter, and S is the shortest tumor diameter. The tumor volume and mouse body weight were recorded every 3 days. After the tumors reached a mean volume of 100 mm^3, the animals were randomly assigned into one of four groups (n=6) and treated with vehicle control, 5 mg/kg osimertinib, 100 mg/kg ABT-263 alone or in combination; both agents were administered by oral gavage daily. At the end of experiment (32 days after implantation of tumor cells), the mice were sacrificed by carbon dioxide asphyxiation with a flow rate of 15% chamber volume/min and the tumors were harvested and weighed.

Immunohistochemistry. The xenograft tumor tissues were immersed in 4% paraformaldehyde for >24 h at room temperature, and transferred to 70% ethanol. Individual lobes of tumor tissues material were placed in processing cassettes, dehydrated through a serial alcohol gradient, and embedded in paraffin wax blocks. Before immunostaining, 5 μm thick xenograft tumor tissue sections were dewaxed in xylene, rehydrated through decreasing concentrations of ethanol and washed in PBS. Then, antigens were unmasked by microwaving sections in 10 mmol/l citrate buffer, pH 6.0 (15 min), and blocked with 5% goat serum (cat. no. SL038; Beijing Solarbio Science & Technology Co., Ltd.) at room temperature for 15 min. Then, immunostaining was undertaken using the avidinbiotinylated enzyme complex method with antibodies against Bcl-2 (1:50 dilution, cat. no. 12789-1-AP; ProteinTech Group, Inc.), Bcl-xL (1:50 dilution, cat. no. 26967-1-AP; ProteinTech Group, Inc.), BimEL (1:50 dilution, cat. no. 22037-1-AP; ProteinTech Group, Inc.) overnight at 4˚C, and equivalent concentrations of polyclonal nonimmune IgG controls. After incubation with the biotin-conjugated secondary antibody (cat. no. GK600705, Gene Tech, Inc.) for 2 h at room temperature and subsequently with streptavidin solution, color development was performed using 3,3-diaminobenzidine tetrahydrochloride (cat. no. P0203; Beyotime Institute of Biotechnology) as a chromogen at room temperature for 1 min. Sections were counterstained using Gill-2 hematoxylin (cat. no. C0107, Beyotime Institute of Biotechnology) at room temperature for 30 sec. After staining, sections were dehydrated through increasing concentrations of ethanol and xylene. The sections were observed and analyzed under a routine light microscope (BX43; Olympus Corporation; magnification, x100 and x200).

Statistical analysis. Statistical analysis was performed using GraphPad Prism software (v5.0; GraphPad Software, Inc.). The IC_{50} values were fitted using a non-linear regression model with a sigmoidal dose response. Results are representative from ≥3 independent experiments and presented as the mean ± SD. Comparisons between the control and treatment groups were determined using a paired Student's t-test or a one-way ANOVA, followed by Tukey's multiple comparison test. P<0.05 was considered to indicate a statistically significant difference. The combination index was calculated using CompuSyn software (v1.0.1; ComboSyn, Inc.) by Chou (20).

Results

Establishment of osimertinib-resistant NSCLC cells. To investigate the molecular mechanism underlying the resistance of NSCLC cells to osimertinib, osimertinib-resistant HCC827 cells (HCC-827/OR) were established through the dosage-escalation of osimertinib over 6 months. The effects of osimertinib on cell viability were analyzed using an MTT assay in HCC827 and HCC-827/OR cells. HCC827 cells were sensitive to osimertinib, demonstrating an IC_{50} value of 35.2 nM, whereas HCC827/OR cells were resistant to osimertinib, exhibiting IC_{50} values of 2.45 μM, ~70-fold larger than sensitive cells (Fig. 1A). The rate of cellular apoptosis induced by osimertinib was determined using Annexin V/PI double staining followed by flow cytometric analysis; the results revealed that osimertinib effectively induced the apoptosis of HCC827 cells in a dose-dependent manner (Fig. 1B and C). Upon treatment with 50, 100 or 200 nM, the total proportion of apoptotic cells (Annexin V-positive staining) increased from 4.7 to 13.0, 21.5 and 37.8%, respectively. In comparison, the treatment of HCC827/OR cells with 1 or 2 μM osimertinib failed to induce apoptosis (Fig. 1D and E). When HCC827/OR cells were treated with 5 μM osimertinib, the total proportion of apoptotic cells (Annexin V-positive staining) was only 18.3%, indicating the resistance of HCC827/OR cells to osimertinib-induced apoptosis.

Bcl-2 and Bcl-xL mediate the resistance of HCC827/OR cells to osimertinib. Since the Bcl-2 protein family is a major regulator of cell apoptosis, the present study investigated whether Bcl-2 and Bcl-xL were involved in the resistance of HCC827/OR cells to osimertinib-induced apoptosis. The results from the western blotting analysis revealed that both the expression levels of Bcl-2 and Bcl-xL were significantly upregulated in HCC827/OR cells (Fig. 2A) compared with HCC827 cells. Subsequently, the expression levels of Bcl-2 and Bcl-xL were knocked down by specific siRNAs in HCC827/OR cells (Fig. 2B and C), respectively, and the rate of osimertinib-induced cellular apoptosis was determined. The osimertinib-induced rate of cellular apoptosis was significantly increased following the knockdown of either

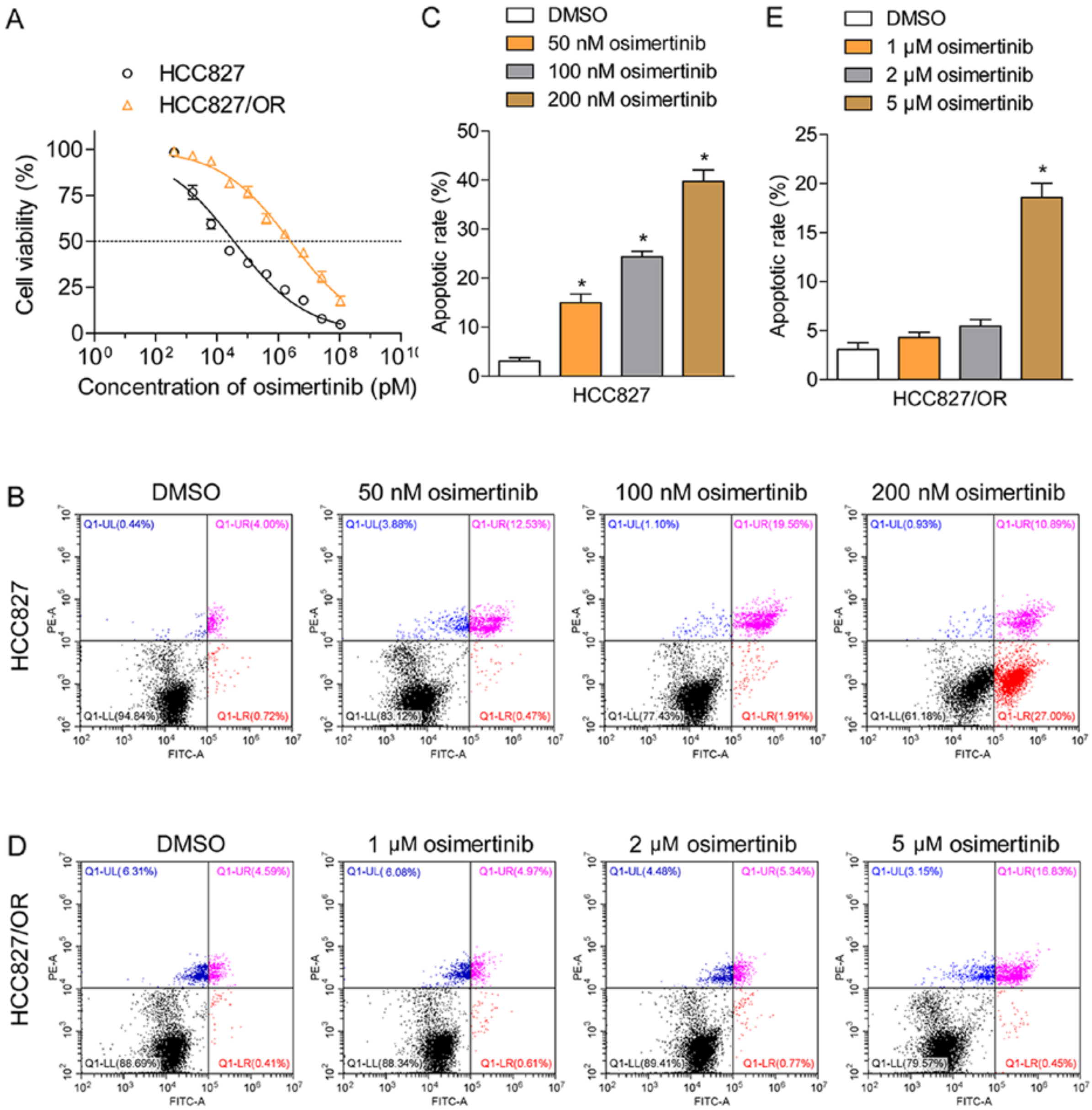

Figure 1. Establishment of osimertinib-resistant non-small cell lung cancer cells. (A) Effects of osimertinib on cell viability were analyzed using an MTT assay in HCC827 and HCC-827/OR cells. (B) Representative profiles of apoptosis induced by osimertinib and (C) quantitative results were obtained using PE/FITC staining in HCC827 cells. (D) Representative profiles of apoptosis induced by osimertinib and (E) quantitative results were obtained using PE/FITC staining in HCC827/OR cells. Data are presented as the mean ± SD from three independent experiments. *P<0.05 vs. DMSO treatment group.

Bcl-2 or Bcl-xL (Fig. 2D-G), indicating that both Bcl-2 and Bcl-xL contributed to the resistance of HCC827/OR cells to osimertinib-induced apoptosis.

Bcl-2/Bcl-xL inhibitor ABT-263 acts in synergy with osimertinib in NSCLS cells. Since the overexpression of Bcl-2 and Bcl-xL were demonstrated to contribute to the resistance of HCC827/OR cells to osimertinib, the present study subsequently investigated whether ABT-263, an inhibitor of Bcl-2 and Bcl-xL, improved the sensitivity of HCC827/OR cells to osimertinib treatment. HCC827/OR cells were treated with a combination of osimertinib and ABT-263 or each individual agent, and cell viability was determined using an MTT assay. The combined treatment with osimertinib and ABT-263 enhanced the inhibition of cell viability compared with the treatment with each single agent alone (Fig. 3A). The combination index (CI) was calculated using the Chou-Talalay method (Fig. 3B), indicating the synergistic effect (CI <1) of osimertinib and ABT-263 in osimertinib-resistant NSCLC cells. In addition, the synergistic effect between osimertinib and ABT-263 in cells was further confirmed using a colony formation assay; the concurrent treatment of HCC827/OR cells with osimertinib and ABT-263 resulted in the enhanced inhibition of colony formation compared with the treatment of cells with either agent alone (Fig. 3C and D).

ABT-263 enhances the rate of cellular apoptosis induced by osimertinib. Cellular apoptosis induced by the combination of osimertinib and ABT-263 or each individual agent were determined using Annexin V-PI double staining. The total number of apoptotic cells (Annexin V-positive staining) induced by the combined treatment of osimertinib and ABT-263 was

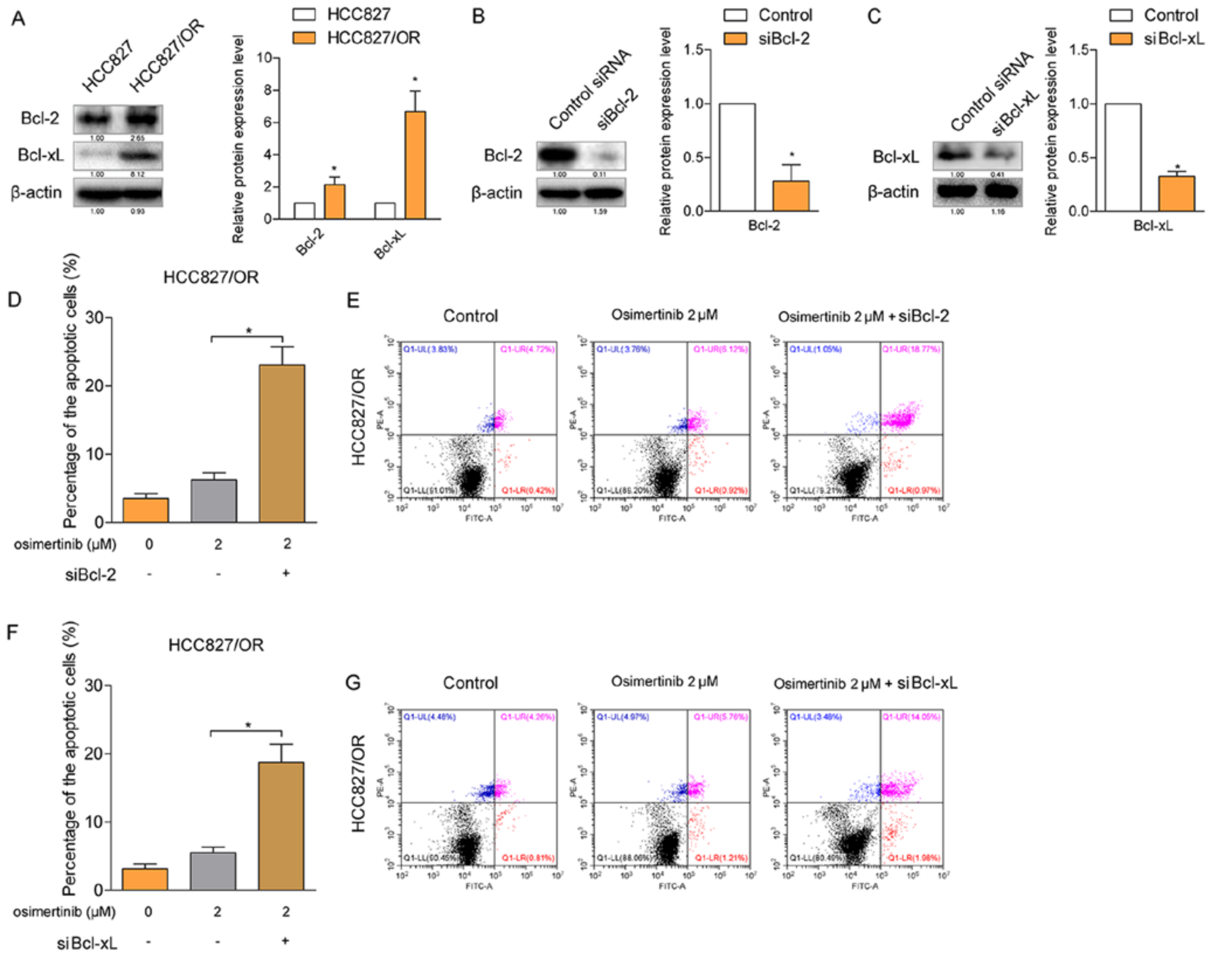

Figure 2. Bcl-2 and Bcl-xL mediated the resistance of HCC827/OR cells to osimertinib. (A) Bcl-2 and Bcl-xL expression levels in HCC827 and HCC-827/OR cells were semi-quantified using western blotting analysis. (B) Bcl-2 and (C) Bcl-xL expression levels were knocked down by specific siRNAs in HCC827/OR cells and semi-quantified using western blotting. Effects of (D and E) Bcl-2 and (F and G) Bcl-xL on osimertinib-induced cellular apoptosis were analyzed using flow cytometry following PE and FITC double staining in HCC827/OR cells. *P<0.05 vs. control group or as indicated. siRNA/si-, small interfering RNA.

significantly increased compared with the number of apoptotic cells induced by each individual agent alone (Fig. 4A and B). To further determine the mechanism of apoptosis induced by osimertinib with ABT-263, protein expression levels were investigated using western blotting in HCC827/OR cells (Fig. 4C and D). The results revealed that, compared with the single agent treatment group, the combined treatment of osimertinib and ABT-263 significantly upregulated the expression levels of BimEL and cytochrome *c*, in addition to promoting the cleavage of caspase-3 and PARP-1. However, the expression levels of Bcl-2 and Bcl-xL were not significantly affected. To further verify whether the function of BimEL was involved in the induction of cellular apoptosis, BimEL was knocked down using siRNA and the knockdown efficiency was confirmed by RT-qPCR (Fig. 4E). The knockdown of BimEL partially attenuated the rate of cellular apoptosis induced by the combined treatment of osimertinib and ABT-263 (Fig. 4F and G), suggesting the contribution of BimEL to the induction of cellular apoptosis. These results indicated that the combined treatment of osimertinib with ABT-263 may enhance the rate of cellular apoptosis through the mitochondria-initiated apoptotic pathway.

ABT-263 enhances antitumor effects of osimertinib in vivo. To investigate the antitumor effects of osimertinib and ABT-263 *in vivo*, a nude mouse subcutaneous tumor model was established using HCC827/OR cells. Treatment of the tumor model mice with either osimertinib or ABT-263 alone led to a slight inhibition of tumor growth compared with the vehicle treated control (Fig. 5A). However, the combination of osimertinib with ABT-263 significantly inhibited tumor growth compared with the single agent treatment groups. At the end of the experiment, the tumors were harvested and weighed. The combined treatment of osimertinib with ABT-263 significantly suppressed tumor growth compared with the single-drug treatment (Fig. 5B), further indicating the potential synergistic antitumor effect of osimertinib and ABT-263 combined. In addition, it was observed that the body weight of osimertinib-treated mice was slightly less compared with ABT-263 treated or vehicle treated mice. However, the difference of body weight among four groups was not significant, suggesting that treatment with the individual agents and the combined use of both agents had slight toxic side effects on the mice (Fig. 5C). It was hypothesized that the osimertinib,

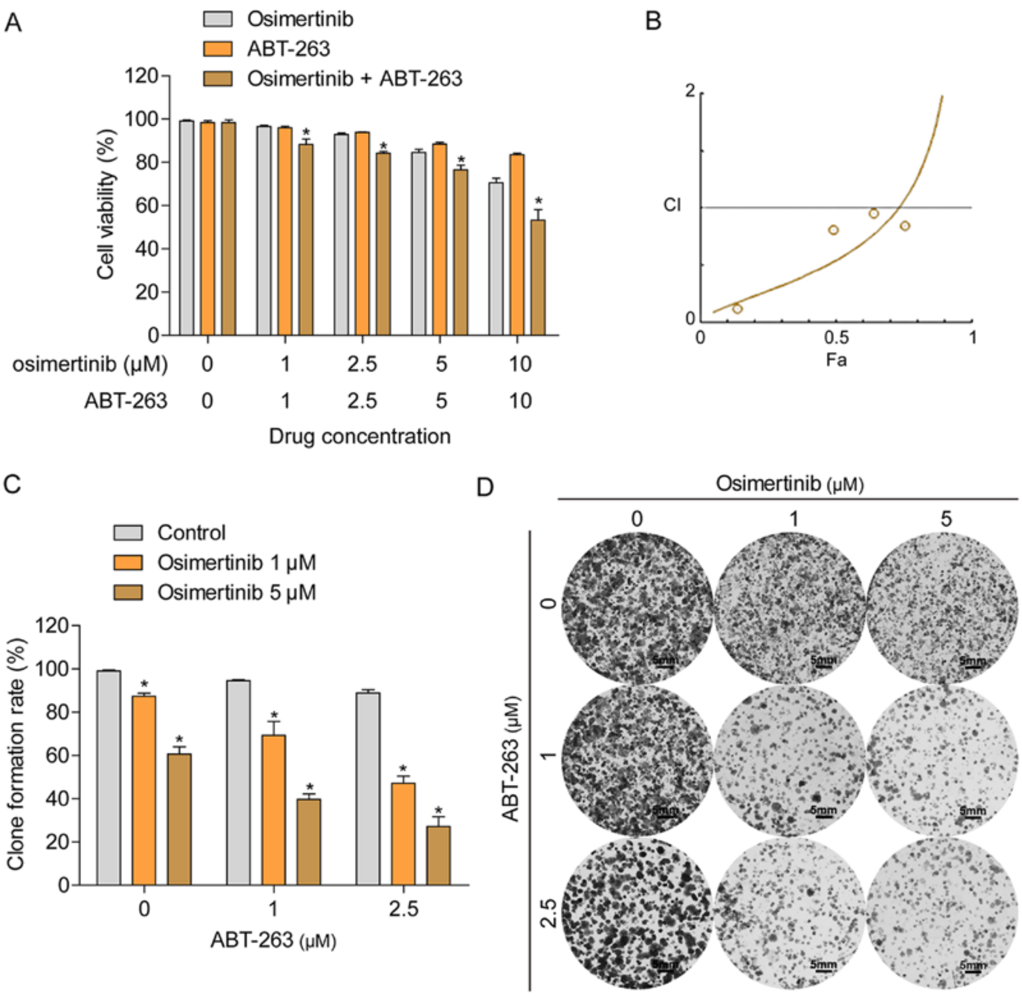

Figure 3. Bcl-2/Bcl-xL inhibitor ABT-263 acts in synergy with osimertinib in non-small cell lung cancer cells. (A) HCC827/OR cells were treated with a combination of osimertinib and ABT-263 or each individual agent and cell viability was determined using a MTT assay. (B) CI of osimertinib and ABT-263 was calculated using the Chou-Talalay method. (C and D) Colony formation assay was used to determine the effects of the concurrent treatment of HCC827/OR cells with both osimertinib and ABT-263. *P<0.05 vs. treatment alone or control group. CI, combination index.

both as single and combined agents, may possess side effect on gastrointestinal tract and affect mice's food intake. The expression levels of Bcl-2, Bcl-xL and BimEL were detected in the xenograft tumor tissues using immunohistochemistry (IHC) (Fig. S1). Consistent with the *in vitro* experiments, the results showed that combined treatment using osimertinib and ABT-263 notably increased the expression of BimEL. However, the expression levels of Bcl-2 and Bcl-xL were but not notably altered. This result indicated that ABT-263 enhanced osimertinib-induced cell apoptosis by elevating BimEL expression.

Discussion

EGFR TKIs have provided a significant benefit for patients with NSCLC harboring EGFR mutations (21); however, the clinical efficacy of TKIs is hindered by acquired resistance (22). Osimertinib, as a third generation TKI, was discovered to overcome resistance to first and second generation TKIs, such as gefitinib, erlotinib and afatinib, by targeting the T790M mutation of EGFR (23-24). However, similar to other TKIs, NSCLC cells eventually develop resistance to osimertinib (25). To identify the underlying mechanism, an osimertinib-resistant cell line HCC827/OR was established through the dosage-escalation of osimertinib over 6 months. Compared with the osimertinib-sensitive HCC827 parent cells, HCC827/OR cells were insensitive to the growth inhibition and apoptosis-induced effects of osimertinib, demonstrating IC_{50} values ~70-fold higher than HCC827 cells.

The inhibition of apoptosis has been identified as one of the major mechanisms involved in the resistance of NSCLC cells to osimertinib (13). Apoptosis is a mechanism of programmed cell death, which is triggered by at least two broad signaling pathways: The extrinsic pathway and the intrinsic pathway. The extrinsic pathway is activated by the interaction between specific ligands and death receptors that belong to the tumor necrosis factor superfamily, subsequently initiating the activation of the caspases cascade to produce proteolysis of essential cell proteins. The intrinsic pathway, also known as the mitochondrial apoptotic pathway, is initiated by the release of cytochrome *c* and other proteins from the mitochondria into the cytosol, inducing the formation of the apoptosome complex and the protease hydrolysis cascade. Bcl-2 family proteins are well-known important regulators of the mitochondrial apoptotic pathway, through keeping the balance between pro- and antiapoptotic proteins. The

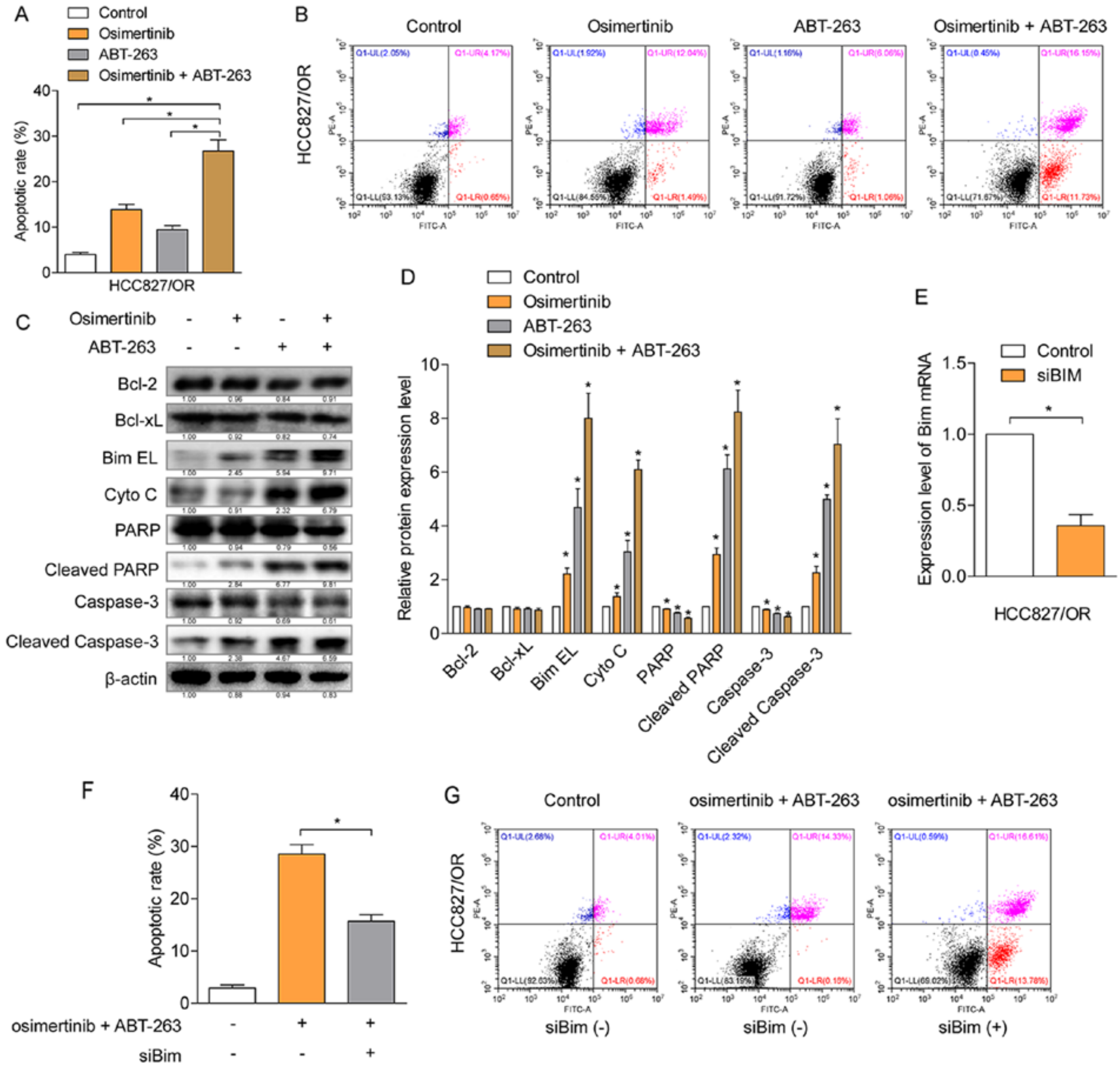

Figure 4. ABT-263 enhances cellular apoptosis induced by osimertinib. (A and B) Rate of cellular apoptosis induced by the combined treatment of osimertinib and ABT-263 or each individual agent was determined using flow cytometry following PE and FITC double staining. (C and D) Cell lysates were evaluated using western blotting analysis in HCC827/OR cells following the treatment with the combination of osimertinib and ABT-263 or each individual agent. (E) Bim expression levels were knocked down by specific siRNAs in HCC827/OR cells and detected using reverse transcription-quantitative PCR. (F and G) Effects of Bim knockdown on cellular apoptosis induced by the combined treatment of osimertinib and ABT-263 were analyzed using flow cytometry following PE and FITC double staining in HCC827/OR cells. *P<0.05 vs. control group or as indicated. siRNA/si-, small interfering RNA; Bim, Bcl-2-like protein 11; cyto *c*, cytochrome *c*; PARP, cleaved poly(ADP-ribose) polymerase 1.

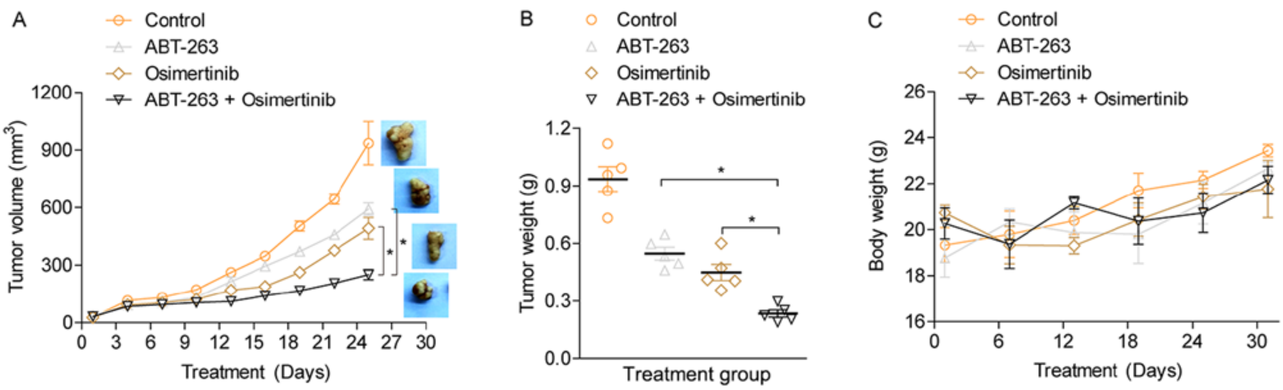

Figure 5. ABT-263 sensitizes tumor cells to the antitumor effects of osimertinib *in vivo*. (A) Antitumor effects of the combined treatment of osimertinib and ABT-263 or each individual agent in a nude mouse subcutaneous tumor model using HCC827/OR cells. (B) Tumor weight of mice following the combined treatment of osimertinib and ABT-263 or each individual agent. (C) Difference in the body weight of mice among each group was analyzed. *P<0.05.

upregulation of antiapoptotic Bcl-2 family members, such as Bcl-2, Bcl-xL and induced myeloid leukemia cell differentiation protein Mcl-1 (Mcl-1), have been identified in a number of solid tumor and leukemia cell lines (26-29). In the present study, Bcl-2 and Bcl-xL expression levels were upregulated in the osimertinib-resistant cell line compared with the sensitive parent cell line. In addition, the downregulation of Bcl-2 or Bcl-xL expression levels by siRNA reversed the drug resistance to osimertinib in HCC8278/OR cells. The downregulation of Bcl-2 was also discovered to overcome the apoptotic inhibition-induced resistance to first generation EGFR TKI gefitinib, as previously reported (14,30), indicating the essential role of Bcl-2 in the resistance of NSCLC cells to EGFR TKIs.

ABT-263 is an orally bioavailable Bcl-2 family inhibitor with a high affinity for Bcl-2 and Bcl-xL (31). Based on the reported role of Bcl-2 and Bcl-xL in the resistance to osimertinib, it was hypothesized that the combination of ABT-263 and osimertinib may overcome the resistance of NSCLC cells to osimertinib. The results of the present study demonstrated that ABT-263 re-sensitized HCC-827/OR cells to osimertinib; the two agents exerted synergistic effects on the inhibition of cell viability and colony formation ability. Moreover, ABT-263 enhanced osimertinib-induced cell apoptosis by elevating BimEL levels and releasing cytochrome *c*, thereby resulting in the cleavage of caspase-3 and PARP-1 (32,33). Bim is another proapoptotic Bcl-2 family member that regulates cell apoptosis through binding to antiapoptotic members, such as Bcl-2 and Mcl-1, and inhibiting their activation, and/or directly activating proapoptoic members, including Bax and Bcl-2 homologous antagonist/killer (34). In the present study, the downregulation of BimEL expression levels by siRNA confirmed the contribution of this protein to the efficacy of osimertinib- and ABT-263-induced apoptosis. Finally, ABT-263 was observed to overcome the resistance of osimertinib in xenograft tumor models and the expression levels of Bcl-2, Bcl-xL and BimEL were also detected by IHC. Consistent with *in vitro* experiments, results from IHC indicated that ABT-263 enhanced osimertinib-induced cell apoptosis through elevating BimEL levels.

As the first third-generation EGFR-TKI in clinical application, osimertinib is primarily used for advanced NSCLC or patients who relapse with poor Eastern Cooperative Oncology Group scores, therefore it is hard to obtain pathological tissues clinically from osimertinib-resistant patients. Hence, one of the limitations of the present study was that the expression of Bcl-2 and Bcl-xL were not determined in the tissues of patients with osimertinib-resistant NSCLC. In the future the tissues of patients with osimertinib-resistant NSCLC will be examined and the results from clinical samples will be reported.

In conclusion, the present study revealed that the expression levels of Bcl-2 and Bcl-xL were upregulated in osimertinib-resistant NSCLC cells compared with sensitive parent cells. In addition, the combined treatment with osimertinib and ABT-263 exerted synergistic inhibition on cell growth, and induced an increased rate of cell apoptosis through the activation of the mitochondrial apoptotic pathway. These findings may provide novel evidence for the development of a combined therapeutic strategy for the treatment of patients resistant to EGFR TKIs.

Acknowledgements

Not applicable.

Funding

The present study was supported by the Scientific Research Foundation from Huadong Hospital (grant no. 2019jc007).

Availability of data and materials

The datasets used and/or analyzed during the current study are available from the corresponding author on reasonable request.

Authors' contributions

YL and ZZ conceived and designed the study. YL, DB and XZ completed molecular and cell biology experiments. YL and HZ performed the *in vivo* study and analyzed the data. YL and ZZ drafted the manuscript. All authors read and approved the final manuscript.

Ethics approval and consent to participate

The animal experimental protocol was approved by the Animal Ethics Committee of Fudan University Shanghai Medical School (Shanghai, China).

Patient consent for publication

Not applicable.

Competing interests

The authors declare that they have no competing interests.

References

1. Bray F, Ferlay J, Soerjomataram I, Siegel RL, Torre LA and Jemal A: Global cancer statistics 2018: GLOBOCAN estimates of incidence and mortality worldwide for 36 cancers in 185 countries. CA Cancer J Clin 68: 394-424, 2018.
2. Torre LA, Siegel RL and Jemal A: Lung cancer statistics. Adv Exp Med Biol 893: 1-19, 2016.
3. Pao W and Chmielecki J: Rational, biologically based treatment of EGFR-mutant non-small-cell lung cancer. Nat Rev Cancer 10: 760-774, 2010.
4. Nan X, Xie C, Yu X and Liu J: EGFR TKI as first-line treatment for patients with advanced EGFR mutation-positive non-small-cell lung cancer. Oncotarget 8: 75712-75726, 2017.
5. Gazdar AF: Activating and resistance mutations of EGFR in non-small-cell lung cancer: Role in clinical response to EGFR tyrosine kinase inhibitors. Oncogene 28 (Suppl 1): S24-S31, 2009.
6. Lee CC, Shiao HY, Wang WC and Hsieh HP: Small-molecule EGFR tyrosine kinase inhibitors for the treatment of cancer. Expert Opin Investig Drugs 23: 1333-1348, 2014.
7. Yu HA, Arcila ME, Rekhtman N, Sima CS, Zakowski MF, Pao W, Kris MG, Miller VA, Ladanyi M and Riely GJ: Analysis of tumor specimens at the time of acquired resistance to EGFR-TKI therapy in 155 patients with EGFR-mutant lung cancers. Clin Cancer Res 19: 2240-2247, 2013.
8. Su KY, Chen HY, Li KC, Kuo ML, Yang JC, Chan WK, Ho BC, Chang GC, Shih JY, Yu SL, *et al*: Pretreatment epidermal growth factor receptor (EGFR) T790M mutation predicts shorter EGFR tyrosine kinase inhibitor response duration in patients with non-small-cell lung cancer. J Clin Oncol 30: 433-440, 2012.

9. Cross DA, Ashton SE, Ghiorghiu S, Eberlein C, Nebhan CA, Spitzler PJ, Orme JP, Finlay MR, Ward RA, Mellor MJ, *et al*: AZD9291, an irreversible EGFR TKI, overcomes T790M-mediated resistance to EGFR inhibitors in lung cancer. Cancer Discov 4: 1046-1061, 2014.
10. Soejima K, Yasuda H and Hirano T: Osimertinib for EGFR T790M mutation-positive non-small cell lung cancer. Expert Rev Clin Phar 10: 31-38, 2017.
11. Thress KS, Paweletz CP, Felip E, Cho BC, Stetson D, Dougherty B, Lai Z, Markovets A, Vivancos A, Kuang Y, *et al*: Acquired EGFR C797S mutation mediates resistance to AZD9291 in non-small cell lung cancer harboring EGFR T790M. Nat Med 21: 560-562, 2015.
12. Ricordel C, Friboulet L, Facchinetti F and Soria JC: Molecular mechanisms of acquired resistance to third-generation EGFR-TKIs in EGFR T790M-mutant lung cancer. Ann Oncol 29 (Suppl 1): i28-i37, 2018.
13. Shi P, Oh Y-T, Deng L, Zhang G, Qian G, Zhang S, Ren H, Wu G, Legendre B Jr, Anderson E, *et al*: Overcoming acquired resistance to AZD9291, a third-generation EGFR inhibitor, through modulation of MEK/ERK-dependent Bim and Mcl-1 degradation. Clin Cancer Res 23: 6567-6579, 2017.
14. Zou M, Xia S, Zhuang L, Han N, Chu Q, Chao T, Peng P, Chen Y, Gui Q and Yu S: Knockdown of the Bcl-2 gene increases sensitivity to EGFR tyrosine kinase inhibitors in the H1975 lung cancer cell line harboring T790M mutation. Int J Oncol 42: 2094-2102, 2013.
15. Nakajima W, Sharma K, Hicks MA, Le N, Brown R, Krystal GW and Harada H: Combination with vorinostat overcomes ABT-263 (navitoclax) resistance of small cell lung cancer. Cancer Biol Ther 17: 27-35, 2016.
16. Emi M, Kim R, Tanabe K, Uchida Y and Toge T: Targeted therapy against Bcl-2-related proteins in breast cancer cells. Breast Cancer Res 7: R940-R952, 2005.
17. Beale PJ, Rogers P, Boxall F, Sharp SY and Kelland LR: BCL-2 family protein expression and platinum drug resistance in ovarian carcinoma. Br J Cancer 82: 436-440, 2000.
18. Mu P, Nagahara S, Makita N, Tarumi Y, Kadomatsu K and Takei Y: Systemic delivery of siRNA specific to tumor mediated by atelocollagen: Combined therapy using siRNA targeting Bcl-xL and cisplatin against prostate cancer. Int J Cancer 125: 2978-2990, 2009.
19. Quadros MR, Connelly S, Kari C, Abrams MT, Wickstrom E and Rodeck U: EGFR-dependent downregulation of Bim in epithelial cells requires MAPK and PKC-delta activities. Cancer Biol Ther 5: 498-504, 2006.
20. Chou TC: Drug combination studies and their synergy quantification using the Chou-Talalay method. Cancer Res 70: 440-446, 2010.
21. Sukrithan V, Deng L, Barbaro A and Cheng H: Emerging drugs for EGFR-mutated non-small cell lung cancer. Expert Opin Emerg Drugs 24: 5-16, 2019.
22. Wu SG and Shih JY: Management of acquired resistance to EGFR TKI-targeted therapy in advanced non-small cell lung cancer. Mol Cancer 17: 38, 2018.
23. Santarpia M, Liguori A, Karachaliou N, Gonzalez-Cao M, Daffinà MG, D'Aveni A, Marabello G, Altavilla G and Rosell R: Osimertinib in the treatment of non-small-cell lung cancer: Design, development and place in therapy. Lung Cancer (Auckl) 8: 109-125, 2017.
24. Bollinger MK, Agnew AS and Mascara GP: Osimertinib: A third-generation tyrosine kinase inhibitor for treatment of epidermal growth factor receptor-mutated non-small cell lung cancer with the acquired Thr790Met mutation. J Oncol Pharm Pract 24: 379-388, 2018.
25. Lazzari C, Gregorc V, Karachaliou N, Rosell R and Santarpia M: Mechanisms of resistance to osimertinib. J Thorac Dis 12: 2851-2858, 2020.
26. Kitada S, Pedersen IM, Schimmer AD and Reed JC: Dysregulation of apoptosis genes in hematopoietic malignancies. Oncogene 21: 3459-3474, 2002.
27. Yamaguchi R, Lartigue L and Perkins G: Targeting Mcl-1 and other Bcl-2 family member proteins in cancer therapy. Pharmacol Ther 195: 13-20, 2019.
28. Faber AC, Farago AF, Costa C, Dastur A, Gomez-Caraballo M, Robbins R, Wagner BL, Rideout WM III, Jakubik CT, Ham J, *et al*: Assessment of ABT-263 activity across a cancer cell line collection leads to a potent combination therapy for small-cell lung cancer. Proc Natl Acad Sci USA 112: E1288-E1296, 2015.
29. Sarosiek KA, Ni Chonghaile T and Letai A: Mitochondria: Gatekeepers of response to chemotherapy. Trends Cell Biol 23: 612-619, 2013.
30. Lu M, Liu B, Xiong H, Wu F, Hu C and Liu P: Trans-3,5,4'-trimethoxystilbene reduced gefitinib resistance in NSCLCs via suppressing MAPK/Akt/Bcl-2 pathway by upregulation of miR-345 and miR-498. J Cell Mol Med 23: 2431-2441, 2019.
31. Tse C, Shoemaker AR, Adickes J, Anderson MG, Chen J, Jin S, Johnson EF, Marsh KC, Mitten MJ, Nimmer P, *et al*: ABT-263: A potent and orally bioavailable Bcl-2 family inhibitor. Cancer Res 68: 3421-3428, 2008.
32. Saelens X, Festjens N, Vande Walle L, van Gurp M, van Loo G and Vandenabeele P: Toxic proteins released from mitochondria in cell death. Oncogene 23: 2861-2874, 2004.
33. Sarosiek KA, Chi X, Bachman JA, Sims JJ, Montero J, Patel L, Flanagan A, Andrews DW, Sorger P and Letai A: BID preferentially activates BAK while BIM preferentially activates BAX, affecting chemotherapy response. Mol Cell 51: 751-765, 2013.
34. Shukla S, Saxena S, Singh BK and Kakkar P: BH3-only protein BIM: An emerging target in chemotherapy. Eur J Cell Biol 96: 728-738, 2017.